# Neuronal Growth: A Bistable Stochastic Process

Timo Betz,* Daryl Lim, and Josef A. Käs
*Institute of Soft Matter Physics, Linnéstrasse 5, 04109 Leipzig, Germany*
(Received 29 November 2005; published 10 March 2006)

The fundamentally stochastic nature of neuronal growth has hardly been addressed in neuroscience. We report on the stochastic fluctuations of a neuronal growth cone's leading edge movement, the basic step in neuronal growth. Describing the edge movement as a stochastic bistable process leads to an isotropic noise parameter that is successfully used to test the model. An analysis of growth cone motility confirms the model, and predicts that linear changes of the bistable potential, as known from stochastic filtering, result in directed growth cone translocation.

DOI: 10.1103/PhysRevLett.96.098103 PACS numbers: 87.17.Jj, 05.10.Gg, 87.19.La, 87.19.St

Neuronal growth is a complex process in which an intriguing machine at the tip of a growing neurite, called the growth cone (Fig. 1), maneuvers itself through a developing organism by integrating chemical and mechanical signals. The motility of these structures is based on the dynamics of a polymer network made up of semiflexible actin filaments, arranged in a sheetlike structure around the center of a growth cone, also known as the lamellipodium [1]. While biologists generally assume a causal relation between the external signaling and the cellular activities, the inherent stochastic nature of biochemical reactions in small subcellular structures is generally neglected. In addition to this internal stochasticity, the randomness of the extremely weak external signals should be considered. It has been demonstrated that the growth cone is able to detect chemical signal gradients as small as a difference of a single molecule across its structure [2], and that such weak signal intensities are very likely to undergo rapid and large fluctuations. This stochastic viewpoint of neuronal growth raises the question of how nature ensures the correct wiring of the central nervous system. Surprisingly, an analysis of the stochastic processes involved in neuronal growth has only been addressed in the context of dynamic instabilities of microtubule and filopodial dynamics [3], while examination of the lamellipodium dynamics of growth cones has not received much attention. Recent works have analyzed the edge dynamics of fibroblasts [4], and focused on detected periodic movements instead of the stochastic fluctuations as found in our experiments on neuronal growth cones.

To gain insight into the stochasticity of neuronal growth, we recorded the growth cone edge evolution of a neuronal cell line (NG108-15), transfected to express fluorescently labeled actin monomers (pEGFP-human-$\beta$-actin [5]) for edge motility visualization. Labeled actin is an effective marker since the lamellipodium is known to be filled with monomeric and filamentous actin [6]. Figure 1 shows a confocal fluorescent image of these growth cones and explains the method used to determine the edge position with subpixel resolution of $\pm 6$ nm. For each growth cone we recorded a 10 min time series with a time lag of 5 sec between images. After Gaussian filtering, the edge position was measured with respect to a pixel based center-of-mass (c.m.) [7]. The edge speed was evaluated by substracting the edge positions of subsequent images. This was done in 500 equally spaced angular directions to obtain the edge speed for each direction. For this, the mean c.m. of both images was used and reevaluated for subsequent image pairs.

Since the edge detection method presented in Fig. 1 relies on an accurate fit, we used the fit parameters and the fit quality to exclude nonreliably detected edge positions. For further analysis, we separate the measured edge

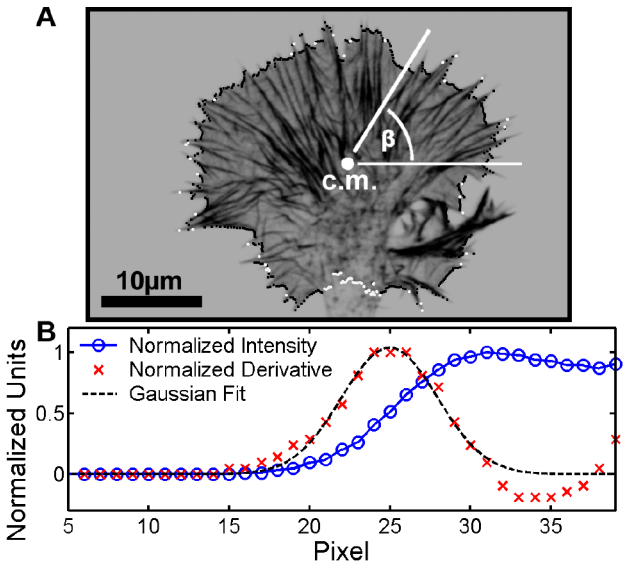


FIG. 1 (color online). (a) Confocal fluorescence image of a GFP-actin transfected neuronal NG108-15 growth cone. The edge position was determined from each image by extracting a line profile along an angle dependent direction taken from the c.m. To get subpixel position resolution, a Gaussian function was fitted to the derivative of each of these line profiles (b). The fit properties were used to determine the reliability of the detection, visualized in (a) by white dots for unreliably detected and black for reliably detected edge positions. The 95% confidence interval for the fit gives an error of $<6$ nm.

 

speed evolution for each direction into distinct growth and retraction phases, with positive and negative speeds, respectively. First, we are interested in the mean velocity distribution of the growth and retraction phases. Throughout our analysis, velocity always denotes the mean velocity within the mentioned phases. Figure 2(a) shows the resulting velocity distribution for a given growth cone, during the whole observation time, and for all acquired angles. The histogram shows that the lamellipodium moves with both a prominent protrusion and retraction velocity. From our experiments on 24 growth cones, we measured an average retraction velocity of $-1.60 \pm 0.55\ \mu\mathrm{m/min}$ and an average protrusion velocity of $1.56 \pm 0.69\ \mu\mathrm{m/min}$. Such a velocity distribution suggests that the growth cone's edge follows a two state process behavior. In order to determine the extent to which the switching between these states is stochastic, we examined the residence time distribution (RTD), which gives the global probability of staying a given time in either a growing or retraction state. The RTD combines the data collected for all directions and over the whole measurement period, and is presented in Fig. 2(b). The logarithmic plot proves an exponential behavior of this distribution, and the exponential fit function gives a surprisingly accurate description of the biological process. The fitted exponential decay values for the presented growth cone are $0.08 \pm 0.01\ \mathrm{s}^{-1}$ and $0.11 \pm 0.01\ \mathrm{s}^{-1}$ for the switch from retraction to protrusion and vice versa.

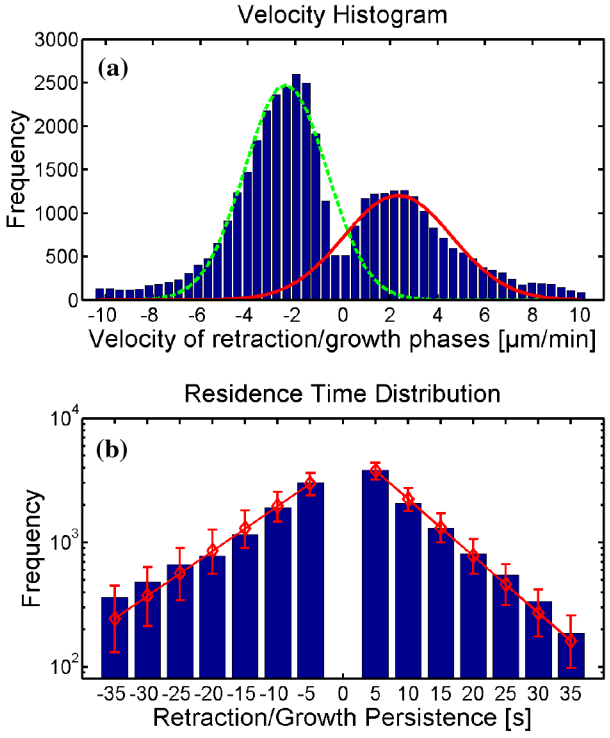


FIG. 2 (color online). Statistics of lamellipodial fluctuations. (a) The measured velocity probability distribution (bars) of a growth cone typically shows two prominent protrusion and retraction velocities. For the fitting of the histogram, we assume a favored protrusion and retraction velocity, influenced by the inherent noise of a biological system. Thus, it is adequate to fit Gaussians to the histograms and we determined the respective maxima at $-2.36 \pm 0.11\ \mu\mathrm{m/min}$ (dotted line) and $2.42 \pm 0.18\ \mu\mathrm{m/min}$ (solid line) with the displayed fits. (b) presents a log plot of the residence time distribution (bars), and an exponential fit-function (solid line) const $\times \exp(-r_M t)$, where $r_M$ denotes the measured decay rate and $t$ time. The decay rates in this example are $0.08 \pm 0.01\ \mathrm{s}^{-1}$ for the retraction and $0.11 \pm 0.01\ \mathrm{s}^{-1}$ for the protrusion. (Errors, and error bars represent the 95% confidence interval for fits used.)

An exponential decay of the RTD is a characteristic of stochastic processes with statistically independent noise, well studied in terms of the famous Kramers problem [8]. The exponential decay was highly reproducible and for both directions we measured decay rates from $0.078 \pm 0.021\ \mathrm{s}^{-1}$ to $0.147 \pm 0.021\ \mathrm{s}^{-1}$. In addition, the accuracy of the fits was excellent, with the $r$-square value always above 0.95. The exponential decay of the RTD shows that the edge velocity switches in a stochastic fashion between the protrusion and the retraction state. A closer look at the RTD presented in Fig. 2(b) shows that the exponential decay of the protrusion states is faster than that of the retraction state. Additionally, the mean velocity distribution shows a significantly sharper peak of the dominant retraction velocities. This behavior was generally observed for the measured growth cone fluctuations, and is reflected in the average decay rate of retractions at $0.096 \pm 0.012\ \mathbf{s^{-1}}$, which is smaller than the average decay rate of protrusions at $0.107 \pm 0.019\ \mathbf{s^{-1}}$. Such a relation between the measured histograms of velocity distribution and of the RTD suggests that both are the result of a bistable stochastic process, well known and studied since Kramers' famous publication [8]. To model the measured probability densities with a bistable stochastic process, and to test this assumption, we started with the following Langevin equation:

$$\frac{dv(t)}{dt} = -\frac{\partial V(v)}{\partial v} + \sqrt{2\eta}\xi(t), \tag{1}$$

where $v(t)$ is the edge velocity at a given time, $V(v)$ is a velocity dependent potential, $\eta$ is the noise parameter, and $\xi(t)$ represents Gaussian white noise with $\langle\xi\rangle = 0$ and $\langle\xi(t)\xi(t+\tau)\rangle = \delta(t-(t+\tau))$. It is important to note, that this is a Langevin equation in velocity space. This is equivalent to a biased random walk whose position is controlling the velocity of the edge. The edge position itself is not directly described by this equation. As described in [9], this Langevin equation leads to the following Fokker-Planck equation:

$$\frac{\partial p(v)}{\partial t} = \frac{\partial}{\partial v}\left[V'(v)p(v)\right] + \eta\frac{\partial^2}{\partial v^2}p(v), \tag{2}$$

where $p(v)$ is the velocity probability distribution. In the cell line used, the macroscopic growth cone parameters like growth direction and translocation speed usually vary on the time scale of 30 to 60 min. Thus, we assume that the

edge velocity statistics do not change during the 10 min measurement period and use the stationary solution ($\frac{\partial p(v)}{\partial t} = 0$) of this Fokker-Planck equation, which relates the potential $V(v)$ and the probability distribution $p(v)$ as follows:

$$p(v) = \text{const} \times \exp\left(-\frac{V(v)}{\eta}\right), \tag{3}$$

where const is a normalization constant. Using the measured velocity probability distribution, we can get the potential by taking the negative ln:

$$\frac{V(v)}{\eta} = -\ln p(v) - \text{const.} \tag{4}$$

Thus, $\frac{V(v)}{\eta}$ is, besides the normalization constant, experimentally measurable. To get a relation between the probability distribution of the velocity [Fig. 2(a)] and the residence time distribution [Fig. 2(b)], we follow Kramers' approach to quantify the decay of a bistable system [8,9]. Kramers relates the decay value of a metastable state to the potential barrier, and to the curvature of the potential at the maxima and the minima of the metastable states [Fig. 3(a): $\alpha, \gamma$] and the unstable state [Fig. 3(a): $\beta$]. Hence, with a given potential $V$, we can get the reduced Kramers rate, i.e., the Kramers decay rate $r_K$, over the noise parameter $\eta$, given by

$$\frac{r_K}{\eta} = \frac{\sqrt{V''(\alpha)|V''(\beta)|}}{2\pi\eta} \exp\left(-\frac{\Delta V}{\eta}\right), \tag{5}$$

where $V''(\alpha)$ and $V''(\beta)$ are the second derivatives of the potential at the metastable state ($\alpha$) and at the instable peak ($\beta$), and $\Delta V$ is the potential difference between these states. The measured mean curvatures of the scaled potential are $V''(\alpha)/\eta = 17.9 \pm 3.1 \times 10^{-3}\ (\frac{\text{min}}{\mu\text{m}})^2$, $V''(\beta)/\eta = -92.9 \pm 27.9 \times 10^{-3}\ (\frac{\text{min}}{\mu\text{m}})^2$, and $V''(\gamma)/\eta = 15.7 \pm 2.5 \times 10^{-3}\ (\frac{\text{min}}{\mu\text{m}})^2$. Using this method, we get a reduced Kramers rate for the switching from a retraction to a protrusion state and vice versa by replacing $V''(\alpha)$ with $V''(\gamma)$ and changing the $\Delta V$ accordingly. Thus, we can now obtain the noise parameter $\eta$, by comparing the measured decay rate $r_M$ of the RTD [Fig. 2(b)] with the reduced Kramers decay rate $\frac{r_K}{\eta}$. Numerically, this gives two independent noise parameters for the transition from a protrusion to a retraction phase $\eta_{\text{pr}}$ and back $\eta_{\text{rp}}$:

$$\eta_{\text{pr}} = \frac{r_{M_{\text{pr}}}}{(\frac{r_K}{\eta})_{\text{pr}}}, \qquad \eta_{\text{rp}} = \frac{r_{M_{\text{rp}}}}{(\frac{r_K}{\eta})_{\text{rp}}}. \tag{6}$$

Applying this model to the measured lamellipodium fluctuations, we can now compute the two noise parameters $\eta_{\text{pr}}$ and $\eta_{\text{rp}}$.

To test if the model of a stochastic driven bistable process is an adequate description for the measured distribution, we can compare the two measured noise parameters with each other. In the case of a stochastic bistable process, the noise parameters should be independent from the switching direction, as the noise should be isotropic. This is physically equivalent to the requirement that the two determined parameters are equal. Indeed, following the described procedure, we found that in 21 out of 24 growth cones, the two noise parameters were equal within the experimental error, as presented in Fig. 3(b). As mentioned before, the physical meaning of this noise parameter is a diffusion constant in velocity space.

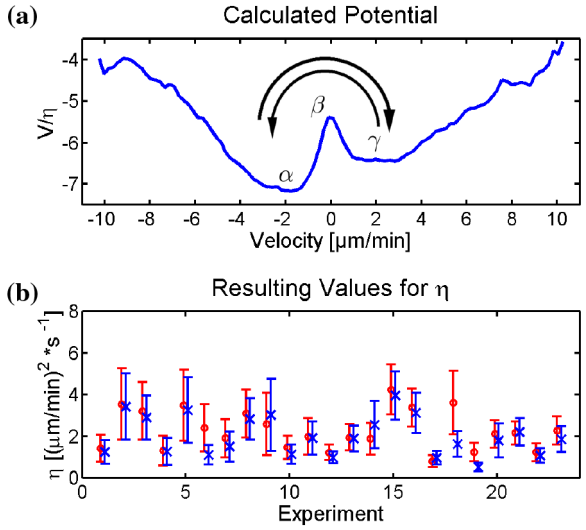


FIG. 3 (color online). (a) Calculated potential using Eq. (4). The arrows visualize the stochastic switching between a retraction (left) and a protrusion (right) state. $\alpha$ and $\gamma$ denote the potential minima, and $\beta$ the potential maxima. The potential can be used to infer the noise parameter for switching from retraction to protrusion and vice versa. (b) The resulting noise parameters for 23 experiments. $\eta_{\text{rp}}$ is presented by a circle and $\eta_{\text{pr}}$ by a cross. [For better readability, one experiment with values $\eta_{\text{rp}} = 16.6 \pm 8.2\ (\frac{\mu\text{m}}{\text{min}})^2\,\text{s}^{-1}$ and $\eta_{\text{pr}} = 15.2 \pm 7.7\ (\frac{\mu\text{m}}{\text{min}})^2\,\text{s}^{-1}$ was omitted in the graph.]

Based on the above, our interpretation is that the experiments reflect the outcome of a bistable stochastic process that controls the polymerization at the leading edge of the lamellipodium. Physically, the forward motion of the lamellipodium depends largely on the polymerization of actin filaments [10], which in turn depends strongly on the actin monomer concentration and free filament ends [11]. The backward motion, however, is not due to depolymerization, but instead depends on the rearward motion of the whole actin network towards the center of the growth cone. This process, known as retrograde flow [12], varies slowly as compared to the aforementioned edge fluctuations. Driven by inherently stochastic myosin motors, the retrograde flow changes slowly since the coupling of the motors through the viscoelastic actin gel only allows a weak correlation, but no processivity. Superimposed on this backward motion, the lamellipodium edge fluctuates on a timescale of seconds, driven by changes in the polymerization speed which results in the measured stochastic behavior. The measurements and the presented model show that the lamellipodium fluctuations of neuronal

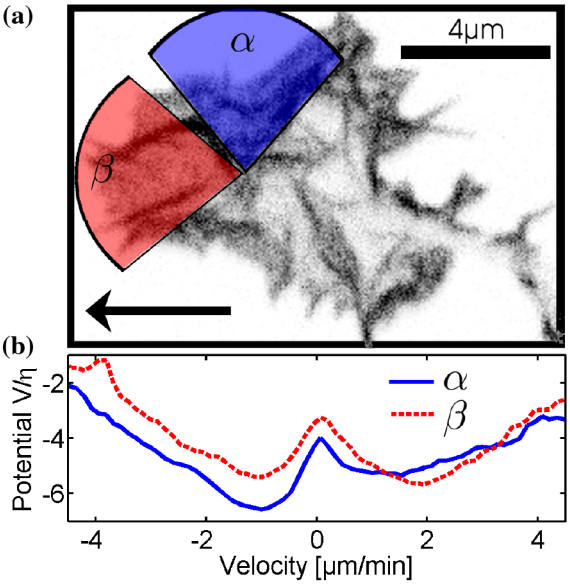


FIG. 4 (color online). (a) Fluorescent image of a GFP-actin transfected growth cone, translocating in the direction of the arrow. The two marked areas, $\alpha$ and $\beta$, are independently analyzed, and the measured potentials are presented in (b). Whereas the potential perpendicular to the direction of growth (solid line) favors the retraction states, the potential in the direction of growth presents a tilted potential that favors the growth of the lamellipodium.

growth cones can be described by a simple bistable stochastic process which controls actin polymerization. Possible molecular mechanisms include an inherent stochastic polymerization rate, a stochastic capping and uncapping of free filament ends, and a fluctuative sequestering of actin monomers.

Since the presented model relates the long-term movement of the growth cone to the statistics of the edge fluctuation, the local potential in the direction of growth should favor growth periods over retraction periods. To test this prediction, we examined a growth cone which translocated over a 10 min measurement period. Figure 4 shows such a growth cone, and presents the potentials for the direction of growth ($\beta$) and the direction perpendicular to growth ($\alpha$). Our analysis shows that in the direction perpendicular to the direction of growth ($\alpha$), retraction is favored. This is illustrated by the slower decay of the retraction states ($5.6 \pm 2.1 \times 10^{-2}\ \mathrm{s}^{-1}$) as compared to the protrusion states ($9.9 \pm 1.4 \times 10^{-2}\ \mathrm{s}^{-1}$). Furthermore, in the direction of growth ($\beta$), the potential is shifted to favor protrusions, and the decay rate of the retraction states ($7.7 \pm 0.8 \times 10^{-2}\ \mathrm{s}^{-1}$) was slightly faster than the decay rate of the protrusion states ($7.1 \pm 1.1 \times 10^{-2}\ \mathrm{s}^{-1}$). The presented Kramers analysis gives noise parameters of $\eta^{\alpha}_{\mathrm{rp}} = 1.32 \pm 0.84\ (\frac{\mu\mathrm{m}}{\mathrm{min}})^2\,\mathrm{s}^{-1}$, $\eta^{\alpha}_{\mathrm{pr}} = 1.36 \pm 0.74\ (\frac{\mu\mathrm{m}}{\mathrm{min}})^2\,\mathrm{s}^{-1}$, $\eta^{\beta}_{\mathrm{rp}} = 1.35 \pm 0.57\ (\frac{\mu\mathrm{m}}{\mathrm{min}})^2\,\mathrm{s}^{-1}$, and $\eta^{\beta}_{\mathrm{pr}} = 2.08 \pm 0.92\ (\frac{\mu\mathrm{m}}{\mathrm{min}})^2\,\mathrm{s}^{-1}$.

As mentioned above, the growth cone has to detect weak signals in a noisy environment, so it is seemingly impossible that signals below the noise level are detectable. To overcome this problem, which is critical for the proper development of an organism, our data allows the hypothesis that nature uses a process known as stochastic filtering or stochastic resonance, that has been originally proposed to explain the periodic recurrences in global climate dynamics [13]. This phenomenon has been examined in detail both theoretically [14] and experimentally [15,16], and it has been shown that it is also applicable to nonperiodic input signals [17]. To utilize this elegant stochastic signal amplification, the cell would have to be able to influence the noise parameter to push the system to the point of maximal sensitivity. The observed changes in measured noise values indicate that this noise tuning may indeed be taking place in the observed neurons.

The authors would like to thank A. Ehrlicher, M. Goegler, and D. Koch for helpful discussions, and Mrs. Marianne Duda and the DFG (KA 1116/3-2) for financial support.

*Electronic address: tobetz@physik.uni-leipzig.de

[1] P. R. Gordon-Weeks, Neuroscience (Oxford) **21**, 977 (1987).
[2] W. J. Rosoff, J. S. Urbach, M. A. Esrick, R. G. McAllister, L. J. Richards, and G. J. Goodhill, Nat. Neurosci. **7**, 678 (2004).
[3] D. J. Odde and H. M. Buettner, Biophys. J. **75**, 1189 (1998).
[4] H. G. Dobereiner, B. Dubin-Thaler, G. Giannone, H. S. Xenias, and M. P. Sheetz, Phys. Rev. Lett. **93**, 108105 (2004).
[5] C. Ballestrem, B. Wehrle-Haller, and B. A. Imhof, J. Cell Sci. **111**, No. 12, 1649 (1998).
[6] K. Sobue, Neurosciences Res. **18**, 91 (1993).
[7] B. Stuhrmann, M. Goegler, T. Betz, A. Ehrlicher, D. Koch, and J. Kas, Rev. Sci. Instrum. **76**, 035105 (2005).
[8] H. A. Kramers, Physica (Amsterdam) **7**, 284 (1940).
[9] C. Gardiner, *Handbook of Stochastic Methods*, Springer Series in Synergetics; [13] (Springer, Berlin, 2004), 3rd ed.
[10] A. Ehrlicher, T. Betz, B. Stuhrmann, D. Koch, V. Milner, M. G. Raizen, and J. Kas, Proc. Natl. Acad. Sci. U.S.A. **99**, 16 024 (2002).
[11] A. Mogilner and G. Oster, Curr. Biol. **13**, R721 (2003).
[12] C. H. Lin and P. Forscher, Neuron **14**, 763 (1995).
[13] R. Benzi, A. Sutera, and A. Vulpiani, J. Phys. A **14**, L453 (1981).
[14] L. Gammaitoni, P. Hänggi, P. Jung, and F. Marchesoni, Rev. Mod. Phys. **70**, 223 (1998).
[15] A. Simon and A. Libchaber, Phys. Rev. Lett. **68**, 3375 (1992).
[16] D. Babic, C. Schmitt, I. Poberaj, and C. Bechinger, Europhys. Lett. **67**, 158 (2004).
[17] J. J. Collins, C. C. Chow, A. C. Capela, and T. T. Imhoff, Phys. Rev. E **54**, 5575 (1996).